***J. Ocean Univ. China*** (Oceanic and Coastal Sea Research)
https://doi.org/10.1007/s11802-025-6168-5
ISSN 1672-5182, 2025 24 (5): 1401-1413
*http://www.ouc.edu.cn/xbywb/*
*E-mail:xbywb@ouc.edu.cn*

# Evaluating the Use of eDNA Metabarcoding for Monitoring Macrofouling Communities in Net Cage Aquaculture in the Yellow Sea

GU Yalan[1)], WANG Jie[1), *], and DONG Yunwei[1), 2)]

1) *Key Laboratory of Mariculture of Ministry of Education*, *Ocean University of China*, *Qingdao* 266003, *China*
2) *Shandong Key Laboratory of Green Mariculture and Smart Fishery*, *Fisheries College*, *Ocean University of China*, *Qingdao* 266003, *China*

(Received February 21, 2025; revised March 27, 2025; accepted April 24, 2025)


**Abstract** Evaluating species composition and dynamic shifts within fouling communities is essential for developing effective strategies to manage biofouling in marine fish aquaculture. The coastal area in the Yellow Sea is a key area for cage aquaculture in China; however, this region faces significant challenges from biofouling organisms. Here, we employed an experimental approach in a filed mesocosm in a net cage aquaculture area in the Yellow Sea, with weekly monitoring of changes in macrofouling species on mesh nets and in the seawater, to assess the utility of water eDNA metabarcoding for identifying macrofoulers. We compared the temporal variation patterns in the composition and diversity of macrofouling communities identified through morphological method as well as *COI* and *18S rRNA* metabarcoding. The results showed that metabarcoding detected the majority of macrofoulers identified through morphological method (64%), and revealed additional species that were overlooked by traditional monitoring approach. Furthermore, the changes in diversity and community composition over sampling dates in *COI* data were generally consistent with those in morphological identification, although a temporal lag existed between these two approaches. A notable shift in the fouling community occurred at the end of June with the appearance of *Ectopleura crocea* and *Caprella* sp., marking a pivotal change in its structure. Future research could focus on developing targeted primers for these key fouling species, which would enhance the efficiency of monitoring efforts.

**Key words** biofouling; eDNA; cage aquaculture; Yellow Sea

## 1 Introduction

Biofouling is one of the most persistent challenges in the development of cage aquaculture (Fitridge *et al*., 2012; Gao and Dong, 2023). An estimated 5% to 10% of the annual value of the aquaculture industry is allocated to addressing issues related to biofouling (Dürr and Watson, 2010). Its pervasive nature imposes multiple ecological and economic burdens. Biofouling by organisms like barnacles and mussels can obstruct water exchange in net cages, affecting oxygen levels and waste removal, which impacts fish growth (Chen *et al*., 2023). Additionally, biofouling increases the risk of disease transmission, as fouling species harbor pathogens (Dürr and Watson, 2010; Fitridge *et al*., 2012). The biomass can also deform cages, increasing maintenance costs and wear (Beveridge, 2004). With the growth of cage aquaculture, it is urgent to develop effective management solutions to cope with biofouling.

Facing the threats by different biofoulers, like algae, sessile invertebrates (*e.g*., Balanus, Ostreidae, Actiniaria), Rotaria, and Protozoa, various antifouling methods are developed in aquaculture to mitigate the negative effects of biofouling, including net cleaning, chemical antifoulants, and biological control (Gao and Dong, 2023). The efficiency of these methods is contingent upon a comprehensive understanding of the biofouling species and their dynamic changes. For example, net cleaning frequency should align with the reproductive cycles of dominant fouling species and larval settlement patterns, which reach the peaks in spring and early summer in temperate seas in northern China (Yan and Cao, 2008; Zhou *et al*., 2021). Biological antifouling, such as co-culturing fish or invertebrates that consume biofoulers (*e.g*., sea urchins and hermit crabs), can reduce fouling by up to 50% in some cases (Ross *et al*., 2004). However, this method is limited by the feeding preferences of the antifouling species. For example, a study in New Zealand found that *Haliotis* and *Cookia* significantly reduced biofouling (>50%), whereas *Turbo* and *Patiriella* had little effect on certain fouling organisms (Atalah *et al*., 2014). Therefore, prior to implementing antifouling measures, it is necessary to have a clear understanding of the fouling species and their shifts, especially considering the significant variability of foul-

* Corresponding author. E-mail: wangjie@ouc.edu.cn

ing organisms across different marine areas.

Traditionally, marine fouling organisms are identified using a stereomicroscope (Salama *et al*., 2018; Subías-Baratau *et al*., 2022). However, the traditional morphological methods are time-consuming, resource-intensive (He *et al*., 2019; Djurhuus *et al*., 2020), and heavily reliant on specialized taxonomic expertise (Zhou *et al*., 2022). These methods are also prone to human error and biases from taxonomists, as well as being limited by a lack of sufficient taxonomic knowledge (Bourlat *et al*., 2013; Lanzén *et al*., 2021). Due to its time-consuming and labor-intensive nature, morphological identification complicates large-scale, long-term biodiversity monitoring (Elbrecht *et al*., 2017; Hanžek *et al*., 2021). This makes it difficult to meet the needs of comprehensive and extensive monitoring (Pawlowski *et al*., 2014; Frontalini *et al*., 2018).

In contrast, environmental DNA (eDNA) metabarcoding offers several advantages over traditional methods, including reduced time and labor requirements, ease of operation, and no dependence on expert taxonomists for species identification (Rees *et al*., 2014; Lanzén *et al*., 2021). This method enables rapid and large-scale identification of biological components in samples. Over the past decade, eDNA metabarcoding has significantly enhanced monitoring capabilities for marine biofoulers (Briand *et al*., 2018; Rey *et al*., 2020). Despite its advantage, there are some challenges for eDNA metabarcoding method, such as PCR primer and sequencing biases, an incomplete reference database, and classification assignment biases (Beng and Corlett, 2020). Although both morphology and eDNA methods have their own limitations, their advantages are complementary. Therefore, integrating both methods for the identification of biofoulers is an effective approach (Ammon *et al*., 2018; Azevedo *et al*., 2020).

The coastal area of the Yellow Sea, a key net cage aquaculture area in China, has seen a continuous expansion in aquaculture scale, reaching a total of 180130 tons in 2023, which accounts for 15.31% of the national net cage aquaculture production (Fishery Bureau of Ministry of Agriculture of the People's Republic of China, 2024). However, this region faces significant challenges from fouling organisms (Yan and Cao, 2008; Zhou *et al*., 2021). Studies have indicated that aquaculture activities in this area are impacted to varying degrees by fouling organisms such as mussels (Yan and Cao, 2008; Yang *et al*., 2016). However, comprehensive research on the main fouling organism taxa and their dynamic changes is still limited. In this study, we aim to use water eDNA metabarcoding method to monitor biofouling organisms around the net cages and compare the efficiency of two molecular markers (*COI* and *18S rRNA*), as well as assess whether it can effectively reflect the species composition and dynamic shift of the fouling community on the nets.

## 2 Materials and Methods

### 2.1 Experimental Design and Sample Collection

This study was carried out in a nearshore cage aquaculture site (35°14.558'N, 119°31.797'E) in the Yellow Sea, in the Donggang District of Rizhao City, Shandong Province. We employed an experimental approach in a filed mesocosm as previously published studies (Fletcher *et al*., 2017; Ammon *et al*., 2018; Azevedo *et al*., 2020), to weekly monitor changes in macrofouling species on mesh nets and in the seawater (Fig.S1a). Briefly, we built experimental nets with black polyethylene (PE) mesh, identical to those used in the cage aquaculture area. Each net was mounted onto a stainless steel square frame measuring 40 cm×40 cm. This study included seven experimental groups, each consisting of three nets connected by stainless steel chains and ropes (Fig.S1b). After the deployment into the seawater, each experimental group–weighted with lead to maintain vertical orientation–had nets positioned at approximate depths of 0.5, 2.5, and 4.5 m (Fig.S1a). On May 23, the seven experimental groups were evenly suspended on the circular floating valve of a net-cage structure (without a netting system). The floating valve was located within the cage aquaculture area, less than 1000 m from the nearest fish cage.

From May 30 to July 20, one of the seven experimental groups was randomly selected each week for morphological identification. All fouling organisms from the three mesh nets within the selected group were collected, placed in plastic bags, and transported to the laboratory at 4 °C. Organisms that could be easily identified were determined and counted within 24 h; specimens that required further identification were preserved in formalin for later analysis and enumeration. The samples were characterized by a team with over 10 years of experience in marine macrobenthic taxonomy, using an optical microscope at ×10, ×40 and ×100 magnifications. Species were identified to the lowest possible taxonomic level based on their morphological characteristics, by consulting the book *An Illustrated Guide to Species in China's Sea* and the World Register of Marine Species (WoRMS).

Seawater samples for eDNA metabarcoding analysis were collected at the mesh net deployment site during each sampling date. Three 1-L seawater samples were respectively collected from three different depths (0.5, 2.5, and 4.5 m) using a plexiglass water collector (Fig.S1a). These samples were transferred into sterile bottles and transported to the laboratory at 4 °C.

### 2.2 Water Filtration, DNA Extraction, Amplification, and Sequencing

Seawater samples were filtered within 12 h of returning to the laboratory. Prior to filtration, samples were thoroughly shaken to ensure proper homogenization. Each 1-L sample was vacuum-filtered onto a 0.22 μm Sterivex Millipore filter membrane, and the membrane was stored at −80 °C until DNA extraction.

Each filter membrane was cut into pieces and immersed in the mixture (containing 0.5 mL CTAB buffer, 2% CTAB, 1.4 mol/L NaCl, 20 mmol/L EDTA, 100 mmol/L Tris-HCl pH 8.0, 0.2% SDS, 30 μL of 20 mg/mL Proteinase K, and 30 μL of 10 mg/mL RNase A), and in-

cubated at 56 °C for 3 h to ensure complete cell lysis. eDNA was then extracted using the modified CTAB method as previously described (Zhang and Lin, 2005). The concentration and quality of eDNA was assessed using 1% agarose gel electrophoresis and NanoDrop spectrophotometer.

Two genetic markers were amplified: an about 300 bp fragment of the mitochondrial *COI* gene and an about 400 bp segment of the V1–V2 region of the *18S rRNA* gene. The primers used for *COI* gene amplification were mlCOIintF and dgHCO2198 (Leray *et al*., 2013), and for the *18S rRNA* gene, primers SSU_F04 and SSU_R22 were applied (Meyer, 2003). PCR reactions were performed in 25 μL volumes with 12.5 μL of 2× Taq PCR Mix (TIANGEN), 1.5 μL DNA template, 1 μL of each primer, and sterilized water. *COI* amplification involved an initial denaturation at 98 °C for 3 min, followed by 35 cycles of 98 °C for 15 s, 52 °C for 30 s, and 72 °C for 45 s, with a final extension at 72 °C for 5 min. For *18S rRNA*, the thermocycling conditions were 98 °C for 30 s, followed by 35 cycles of 98 °C for 10 s, 57 °C for 30 s, and 72 °C for 30 s, with a final extension at 72 °C for 10 min. PCR products were confirmed by 1% agarose gel electrophoresis, and sequencing libraries were prepared using the NEBNext Ultra II DNA Library Prep Kit (Cat. No. E7645B) and sequenced on the Novaseq 6000 platform (Illumina, PE250).

### 2.3 Bioinformatic Analyses

We used the EasyAmplicon pipeline to analyze eDNA data (Liu *et al*., 2023). Primer sequences and low-quality reads (parameter: *--fastq_maxee_rate* 0.01) were trimmed using the *--fastx_filter* command, and paired reads were merged into single sequences using the *--fastq_mergepairs* in VSEARCH (v2.15.2) (Rognes *et al*., 2016). Redundant sequences were removed using the *derep_fulllength* in VSEARCH, and the data were denoised with the unoise3 algorithm in USEARCH (Edgar, 2016) using the parameter *minsize*>10 to filter out low-abundance noise. Subsequently, chimeric sequences were identified and removed from the denoised sequences using the *uchime_ref*, with the BOLD database for *COI* and the PR2 database for *18S rRNA* sequences serving as reference databases. Finally, the quality-controlled sequences were clustered at 97% similarity to generate the original amplicon sequence variants (ASVs) table.

### 2.4 Reference Database Construction and Species Annotation

To improve species annotation accuracy, we constructed a reference database containing *COI* and *18S rRNA* gene sequences for macrobenthos reported in China, following previously published methods (Castro-Cubillos *et al*., 2022; Fleming, 2023; Pinna *et al*., 2024). First, we compiled a macrobenthos species list using information from the book *Marine Macrobenthic Organisms in China: Research and Practice*. Corresponding *COI* and *18S rRNA* sequences were retrieved from publicly available databases (*e.g*., NCBI, BOLD Systems, and PR2). Only sequences with appropriate length were included: *COI* sequences were typically between 600 bp and 700 bp, and *18S rRNA* sequence ranged from 33 bp to 94 Mb. To ensure the accuracy of species names and taxonomic information, we cross-checked and corrected annotations of the quality-controlled sequences using the WoRMS and the latest taxonomic literature. At the family level, the self-constructed *COI* and *18S rRNA* databases covered 85.47% and 75.58% of the macrobenthic species reported in the Yellow Sea, respectively (please see Supplementary materials 1, 2, and 3 for detailed database information). Representative ASV sequences from the ASV table were then aligned to the reference database using blastn v2.15.0 with the following parameters: blastn -query test.fa -db macrobenthos -outfmt 6 -evalue 1e-5 -max_target_seqs 1 -num_threads 1 -out result.txt. This resulted in a comprehensive annotation table for macrobenthos species. To identify fouling organisms, a list of fouling animals in China was compiled based on the book *Marine Fouling and Its Prevention* and recent surveys from literature. We then compared the macrobenthos annotation table with the fouling species list, generating a macrofouling species annotation table.

### 2.5 Statistical Analyses

Morphological identification data from 21 nets (3 nets per sampling date×7 sampling dates) were used for statistical analysis, while 162 eDNA samples (3 depths×3 replicates per depth×9 sampling dates×2 molecular markers) were included in the statistical analyses. We performed diversity and community structural analyses on both morphologically identified fouling organisms and the annotated fouling organism sequences obtained from eDNA. Alpha diversity was evaluated using the Shannon-Wiener index, Simpson index, Pielou evenness index, and Margalef richness index, which were calculated using the 'vegan' package (Oksanen *et al*., 2022) in R 4.4.0 software (R Core Team, 2024). To assess differences in alpha diversity among sampling dates, Kruskal-Wallis non-parametric tests were performed using the 'rstatix' package (Kassambara, 2023) in R. Generalized liner model (GLM) was employed to assess the effects of sampling date and depth on alpha diversity with a Gaussian distribution in R with 'MASS' package. Beta diversity was quantified using Bray-Curtis dissimilarity, and Principal Coordinate Analysis (PCoA) was used to evaluate variations in community structure among sampling dates. Both Bray-Curtis dissimilarities and PCoA were performed using the *vegdist* and *cmdscale* functions in the 'vegan' package. The significance of differences between dates was tested through Permutational Multivariate Analysis of Variance (PERMANOVA) using the *adonis2* function in the 'vegan' package. Additionally, the average contribution of individual fouling species to within-group similarity and between-group dissimilarity was determined using Similarity Percentage (SIMPER) analysis with Past 4.03 software.

Following the method of Algueró-Muñiz *et al*. (2024), we compared the detection sensitivity of the morphologi-

cal method with that of each genetic markers (*COI* and *18S rRNA*) by examining the taxa identified by both approaches on the same sampling dates. Specifically, for each taxon detected by both methods, we calculated the proportion of samples in which the taxon was identified by only one of the two methods relative to the total number of samples. This metric reflects the degree of congruence between the two methods for each taxon. Additionally, we calculated the ratio of the number of samples identified by the morphological method to those identified by each molecular marker for each taxon, and evaluated the relative detection capacity of the morphological method compared to metabarcoding analysis method employing *COI* and *18S rRNA* sequences.

## 3 Results

### 3.1 Morphological Identification of Biofouling Species

We identified 19 different taxa, belonging to 7 phyla, 9 classes, 10 orders, 13 families, 15 genera, and 14 species (Fig.1a, Table 1). In this study, we did not include the number of *Ectopleura crocea* (Cnidaria) individuals in the subsequent statistical analyses because of two main considerations. First, the individuals of this species were fragile, and it was difficult to obtain intact specimens when removing them from the mesh nets, making it impossible to ensure accurate counts. Second, the abundance of *E. crocea* was so high that it could potentially bias the results of the statistical analyses. For example, in one of the mesh nets, *E. crocea* accounted for 99.60% of the total number of Cnidaria individuals. After excluding *E. crocea*, the most abundant phyla were Arthropoda (95.79%) and Mollusca (2.52%), which dominated throughout the study period (Fig.1b, Fig.2a). Between May 30 and June 13, only a few individuals of certain species, including *Caprella* sp., *Jassa marmorata*, and *Mytilus edulis*, were found on the bare nets (Fig.2b, Fig.S1c, Table S1). After June 13, the nets were increasingly colonized by hydrozoans, while the numbers of other species, such as *Ampithoe valida*, *Stenothoe valida*, and *Nereis multignatha*, also increased.

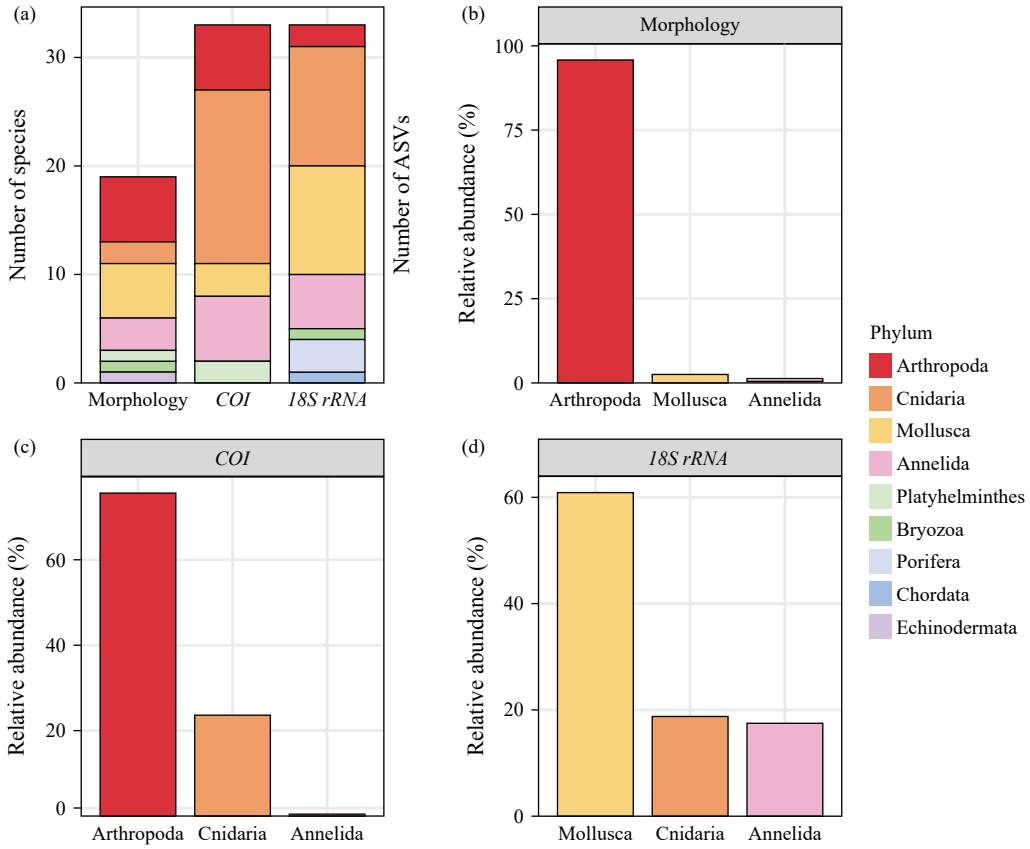


Fig.1 (a) Overview of the total amplicon sequence variants (ASVs)/species obtained from morphology, *COI*, and *18S rRNA*. The relative abundance of the three most numerous phyla in morphology (b), *COI* (c), and *18S rRNA* (d).

Table 1 Taxonomic assignment of biofouling to morphology and different metabarcoding datasets

| | ASVs | Phylum | Class | Order | Family | Genus | Species |
|---|---|---|---|---|---|---|---|
| Morphology | – | 7 | 9 | 10 | 13 | 15 | 14 |
| *COI* | 33 | 5 | 7 | 11 | 13 | 15 | 17 |
| *18S rRNA* | 33 | 7 | 7 | 12 | 17 | 19 | 19 |
| *COI+18S rRNA* | – | 8 | 10 | 18 | 25 | 30 | 32 |
| All | – | 9 | 12 | 20 | 29 | 35 | 37 |

Note: –, not applicable.

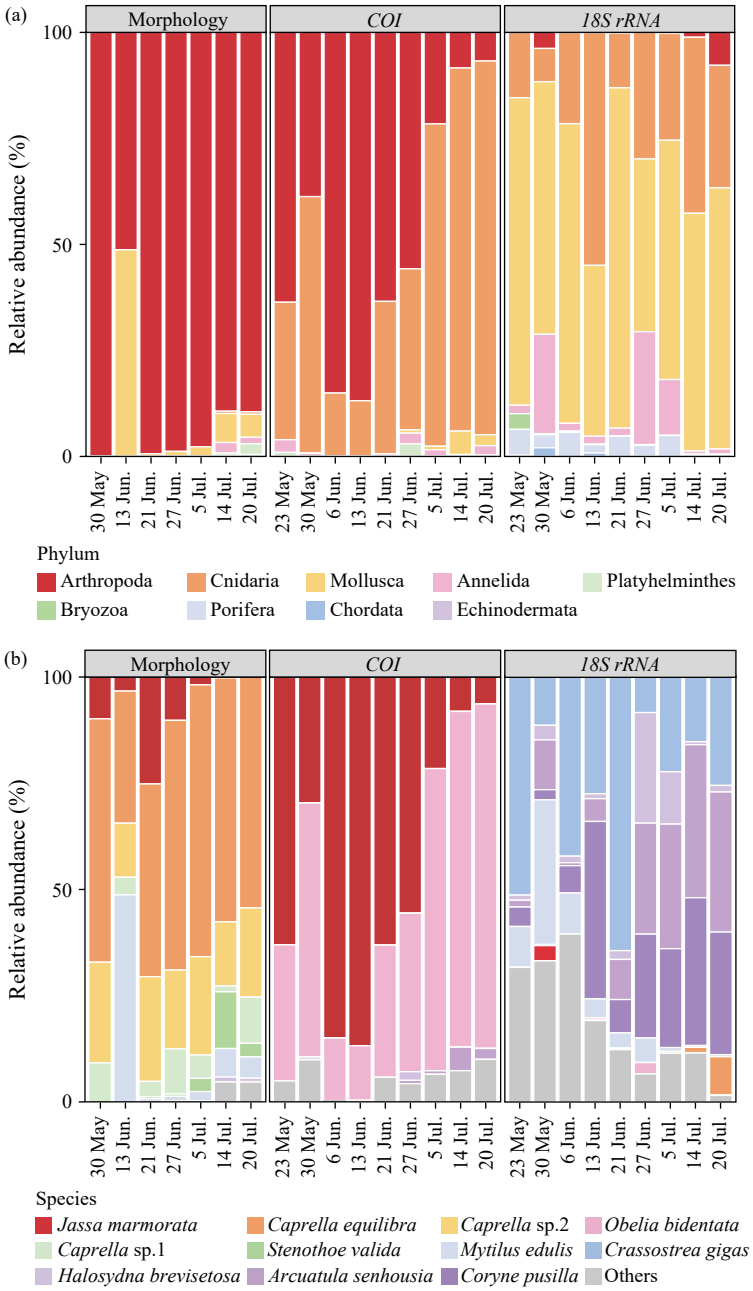


Fig.2 Relative abundance of biofouling taxa at the phylum level (a) and the species level (b) for morphology, *COI* gene, and *18S rRNA* gene.

### 3.2 Biofouler Identification Based on Metabarcoding Analysis

For the *COI* gene, the initial number of raw sequences was 8515499, while for the *18S rRNA* gene, it was 8553505. After applying stringent filtering procedures, we obtained 8162322 high-quality reads for *COI* and 8325211 for *18S rRNA*. Sequence clustering at 97% similarity yielded 1876 ASVs for *COI* and 1371 ASVs for *18S rRNA*, accounting for 8090920 and 8072505 reads, respectively (Table S2). The average read length was 378 bp for *COI* and 414 bp for *18S rRNA*.

Using a self-constructed macrobenthos database, we classified about 84.00% (1575 of 1876 ASVs) of the *COI* data and 60.76% (833 of 1371 ASVs) of the *18S rRNA* data as macrobenthos. When compared to the Chinese nearshore marine fouling database, 33 ASVs were identified as macrofouling in both *COI* and *18S rRNA* (Table S2).

The two markers identified different numbers of macrofouling taxa across taxonomic levels. Of the 33 ASVs identified by *COI*, 5 phyla were represented, covering 7 classes, 11 orders, 13 families, 15 genera, and 17 species (Fig.1a, Table 1). For the 33 ASVs identified by *18S rRNA*, 7 phyla were represented across 7 classes, 12 orders, 17 families, 19 genera, and 19 species. The two markers totally identified 8 phyla, 10 classes, 18 orders, 25 families, 30 genera, and 32 species.

The most abundant phylum identified by *COI* were Arthropoda (75.61%), followed by Cnidaria (23.62%) (Fig.1b). For *18S rRNA*, Mollusca (60.89%), Cnidaria (18.77%) and Annelida (17.49%) were the most abundant phyla. The most abundant species identified varied across

methods: *Caprella equilibra*, *Caprella* sp.1, and *Caprella* sp.2 (Arthropoda) were most abundant in morphological identification, while *Jassa marmorata* (Arthropoda), *Obelia bidentata* (Cnidaria), and *Metridium senile* (Cnidaria) were most abundant by *COI* gene identification (Fig.2b). The most abundant species identified by *18S rRNA* were *Crassostrea gigas* (Mollusca), *Arcuatula senhousia* (Mollusca), and *Halosydna brevisetosa* (Annelida). For *COI*, the abundance of Arthropoda decreased initially (May 23 to 30), then increased (June 6 to 13), and then decreased again (June 21 to July 20) (Fig.2b). In contrast, Cnidaria abundance initially increased (May 23 to June 6) and then decreased (June 13 to July 20). The abundance patterns of dominant phyla in the *18S rRNA* were different. Mollusca and Cnidaria exhibited cyclical fluctuations, with Mollusca initially decreasing and then increasing, while Cnidaria increased before June 13 and later fluctuated cyclically. In contrast, the abundance of Annelida followed a pattern of initial increase (May 23 to 30), then decrease (June 6), then subsequent increase (June 13 to 27), and a final decrease (July 5 to 20).

At the phylum level, both genetic markers identified 5 shared phyla (Fig.3, Table S3). Five phyla detected by *COI* were fully represented by those identified through morphology. Three phyla were exclusively detected by a single method: two by *18S rRNA* and one by morphological identification, with no exclusive phyla detected by *COI*. The percentages of shared taxa identified by the three methods at different taxonomic levels were 33.33% at the class level, 20.00% at the order level, 13.80% at the family level, 8.57% at the genus level, and 8.11% at the species level (Families, genera, and species not identified by morphology were excluded) (Fig.3).

### 3.3 Differences in Detection Sensitivity Between Morphological and Metabarcoding Methods

There were differences in detection sensitivity between morphological and metabarcoding methods, with certain taxa detected exclusively by one method while remaining undetected by another (Tables S4 and S5). In the comparison between morphology and *COI*, *Ectopleura*, *Jassa*, and

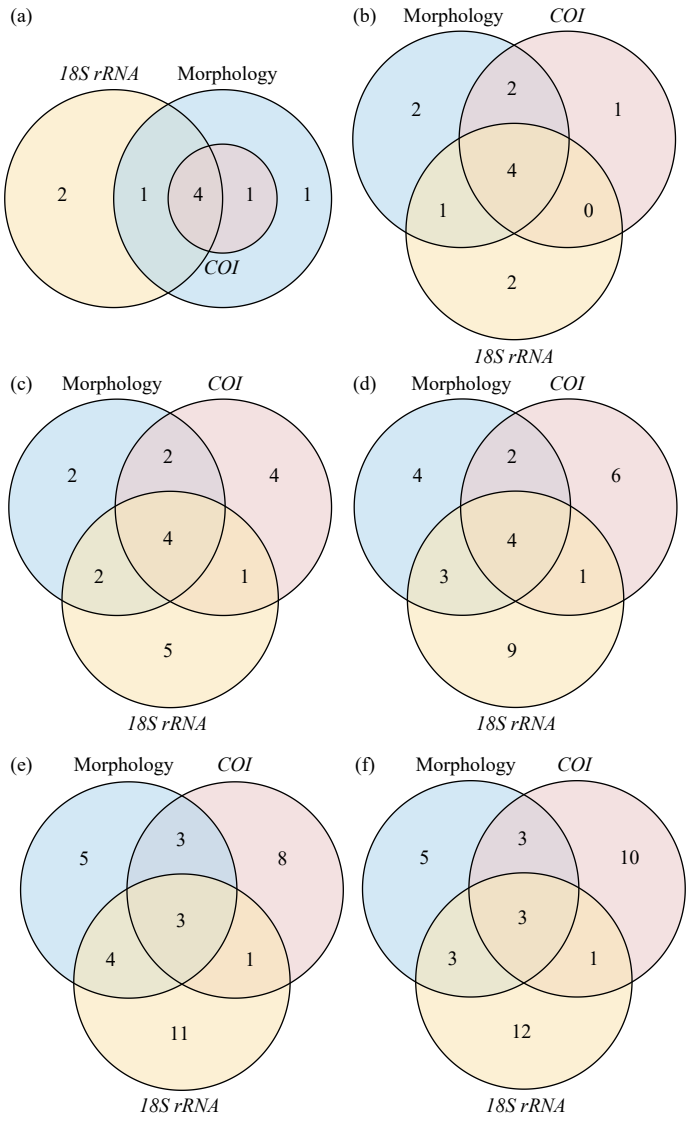


Fig.3 Venn diagram showing the shared and unique biofouling taxa recovered by morphology and gene markers (*COI* and *18S rRNA*) at different taxonomic levels, including (a) phylum, (b) class, (c) order, (d) family, (e) genus, (f) species.

*Nereis* exhibited complete congruency across all sampling dates (with a discrepancy rate of 0%), whereas *Halosydna* showed the highest discrepancy rate, reaching 86%. In the comparison between morphology and *18S rRNA*, the discrepancy rates for *Caprella* and *Mytilus* were 14%, while *Membranipora* displayed a discrepancy rate of 100%. For the taxa detected by both methods, we further compared their relative detection sensitivity by calculating the ratio of the number of samples in which each taxon was detected by one method relative to the other (Tables S4 and S5). The results indicated that most taxa–including *Arcuatula*, *Halosydna*, *Planocera*, *Membranipora*, and *Musculus*–exhibited higher detection sensitivity in eDNA-based analyses. For certain taxa such as *Caprella*, the morphological method demonstrated superior detection capability.

### 3.4 Diversity Analyses and Temporal Variation of the Most Abundant Groups

The temporal variation patterns in diversity indices differed across the morphological, *COI*, and *18S rRNA* datasets. For the morphological data, although no significant differences were observed in the temporal changes of the Shannon and Inverse-Simpson diversity indices, a trend of initial increase (May 30 to June 21), followed by a decrease (June 27 to July 5), and then a subsequent increase (July 14 to 20) was observed (Figs.4a, 4b). The Margalef index showed a trend of decreasing (May 30 to July 5), followed by a slight increase (July 14 to 20) (Fig.4c). The Pielou index revealed a significant change in species richness over time ($H$=18.216, $df$=6, $p$=0.006), with a trend of initial stability (May 30 to June 27) followed by an increase (July 5 to 20) (Fig.4d).

For the *COI* data, the Shannon, Inverse-Simpson, and Pielou indices exhibited significant temporal changes ($p$<0.05), with a trend of initial decrease (May 21 to June 13), followed by an increase (June 21 to July 5), and eventually stabilized (July 14 to 20) (Figs.4e–g). The Margalef index displayed a pattern where species richness remained stable (May 21 to June 13) before beginning to increase (June 21 to July 20) (Fig.4h). For the *18S rRNA* data, no significant differences were observed in any of the diversity indices across the study period, showing an M-shaped fluctuation trend (Figs.4i–l).

GLM results indicated that sampling date significantly influenced the Margalef ($p$<0.001) and Pielou indices ($p$<0.01 in morphology, $p$<0.05 in *COI*) in both morphological and *COI* datasets. In the *COI* dataset, the Shannon ($p$<0.01) and Inverse-Simpson ($p$<0.05) indices were also significantly affected (Table S6).

In the PCoA analysis, inconsistent clustering patterns were observed across the three methods. For the morphological data, two groups were observed: one group from May 30 to June 13, and the other one from June 21 to July 20. These two groups were separated along the PCoA1 axis, which explained 70% of the total variance (Fig.5a). For the *COI* data, all samples clustered into three groups: the first group from May 23 to June 6, the second from June 13 to 27, and the third from July 5 to 20. The first and third groups were separated along the PCoA1 axis, while both the first and third groups were separated from the second group along the PCoA2 axis. The variances that can be explained for these two axes were 46.75% and 20.94%, respectively (Fig.5b). For the *18S rRNA* data, although no distinct grouping was observed, a gradual transition from the start of the experiment (May 23) to the end (July 20) was evident (Fig.5c). The PERMANOVA results confirmed significant differences in community structure across sampling times ($p$=0.001).

SIMPER analysis was performed to assess the contribution of each species to the differences in community composition across sampling time points (Table 2). In the morphological analysis, the top three species contributing to community variation were *Caprella equilibra* (28.47%), *Mytilus edulis* (22.62%), and *Jassa marmorata* (14.11%). For the *COI* gene, community variation was primarily driven by differences in the relative abundance of *Jassa marmorata* (45.24%) and *Obelia bidentata* (40.79%). For the *18S rRNA* gene, *Crassostrea gigas* (20.01%), *Coryne pusilla* (16.12%), and *Arcuatula senhousia* (15.15%) played significant roles in community variation.

## 4 Discussion

Assessing species composition and dynamic changes of fouling communities is a crucial prerequisite for developing effective biofouling management strategies in marine net cage aquaculture. In this study, we evaluated the effectiveness of water eDNA metabarcoding in identifying macrofoulers in a net cage aquaculture area in the Yellow Sea. We found that metabarcoding not only detected most of the macrofoulers identified by morphology (64%, *i.e.*, 9 out of 14 species) at the species level, but also uncovered many species missed by traditional monitoring (23 out of 32 species). There were also differences in species identification between *COI* and *18S rRNA* markers. Additionally, there was a delayed or lagged effect of species diversity between morphology and *COI*-comparison data.

### 4.1 Macrofouler Components Identified by Different Approaches

Metabarcoding detected the same dominant phyla as those through morphological identification. Both methods showed that Arthropoda, Cnidaria, and Mollusca were the main abundant phyla attached to the soft nets. With increasing taxonomic resolution, the overlap in species identified by morphological and metabarcoding methods decreased. At the species level, 9 species were detected by both morphological and metabarcoding approaches (accounting for 64% of morphologically identified species), while eDNA method found other 23 species that were missed by traditional monitoring. Our findings support the results of previous studies (Zaiko *et al*., 2016; Briand *et al*., 2018; Azevedo *et al*., 2020), which showed that traditional and molecular approaches were consistent at high taxonomic levels, while metabarcoding was able to identify a

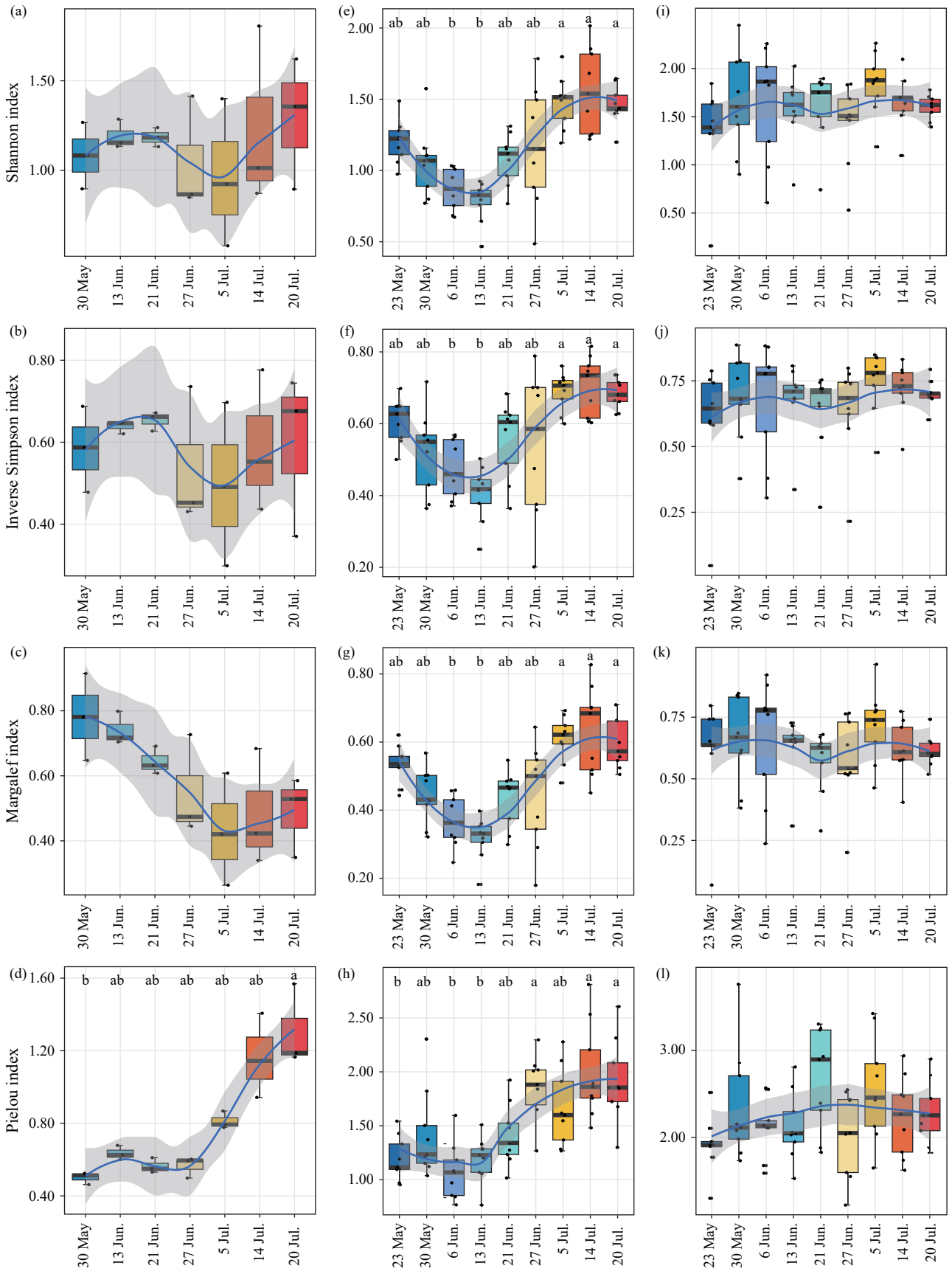


Fig.4 The alpha diversity indices of morphology (a–d), *COI* (e–h) and *18S rRNA* (i–l) at different sampling dates.

much broader range of taxa at lower levels (*e.g.*, genera, species). The sensitivity of morphological and metabarcoding methods also differed. While both methods demonstrated high congruency for several dominant fouling species, such as *Ectopleura*, *Jassa*, and *Caprella*, eDNA generally showed greater sensitivity in detecting the majority of taxa, such as *Arcuatula*, *Halosydna*, *Planocera*, *Membranipora*, and *Musculus*.

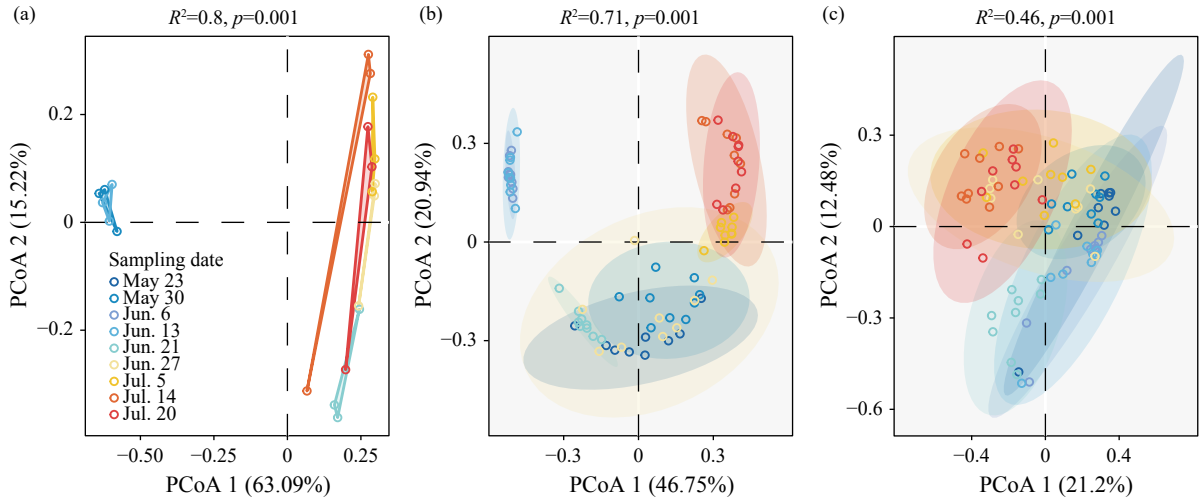


Fig.5 Structure of biofouling community in (a) morphology, (b) *COI*, (c) *18S rRNA* using principal coordinate analysis (PCoA) based on the Bray-Curtis difference index.

Table 2 Contributions of various species/ASVs to biofouling community difference as indicated by SIMPER analysis

| | Species | Contribution (%) | *SD* |
|---|---|---|---|
| Morphology | *Caprella equilibra* | 28.47 | 0.102 |
| | *Mytilus edulis* | 22.62 | 0.163 |
| | *Jassa marmorata* | 14.11 | 0.083 |
| | *Caprella* sp.2 | 12.36 | 0.042 |
| | *Caprella* sp.1 | 11.35 | 0.035 |
| | *Stenothoe valida* | 6.68 | 0.045 |
| *COI* | *Jassa marmorata* | 45.24 | 0.293 |
| | *Obelia bidentata* | 40.79 | 0.252 |
| *18S rRNA* | *Crassostrea gigas* | 20.01 | 0.162 |
| | *Coryne pusilla* | 16.12 | 0.132 |
| | *Arcuatula senhousia* | 15.15 | 0.119 |
| | *Mytilus edulis* | 9.87 | 0.098 |
| | *Halosydna brevisetosa* | 7.40 | 0.079 |
| | *Pennaria disticha* | 6.72 | 0.048 |
| | *Pinna muricata* | 5.10 | 0.039 |

Note: Only species/ASVs with a contribution >5% are shown.

The failure of metabarcoding to identify 36% of the morphologically identified species may be associated with the following factors: i) the DNA of target species may have been diluted or dispersed by water movement, resulting in the absence of their genetic material in the collected samples; ii) degradation of target species' DNA may have occurred, reducing its detectability; iii) the DNA concentration of target species may have been too low, leading to insufficient primer amplification efficiency and, consequently, affecting detection outcomes (Rees *et al.*, 2014; Roussel *et al.*, 2015); iv) the incompleteness of reference databases, particularly the lack of sequence data for certain species, may have limited the accuracy of taxonomic assignment; and v) potential amplification bias during PCR, which could result in the failure to amplify target species or misidentification during database matching (Cowart *et al.*, 2015).

Here, we observed significant difference in the major phyla and species identified by *COI* and *18S rRNA*, respectively. Differences in species identification among molecular markers are primarily influenced by primer amplification bias, variations in the evolutionary rates of target gene regions, the completeness of reference databases, and the taxonomic resolution of different markers (Hajibabaei *et al.*, 2019; Kelly *et al.*, 2019; van der Loos and Nijland, 2021). Among the potential reasons, the sensitivity of molecular markers is likely the most significant factor, as it directly affects the determination of fouling community composition, as well as community diversity and structure (Deiner *et al.*, 2016; Portas *et al.*, 2022). Therefore, to achieve a more comprehensive monitoring of fouling species, it is important to combine multiple molecular markers.

The most abundant macrofoulers are often the key species that affect the service life of net cages and the efficiency of aquaculture operations. Therefore, whether metabarcoding technology can accurately identify the dominant local macrofoulers is a critical factor determining the applicability and widespread adoption of this method. The top abundant species identified by *COI* and *18S rRNA* did not correspond to the species with the highest abundance observed in morphology in the present study. *Ectopleura crocea* (Cnidaria) and *Caprella* sp. (Arthropoda) were most abundant in morphological identification, whereas *Jassa marmorata* (Arthropoda), *Obelia bidentata* (Cnidaria), and *Metridium senile* (Cnidaria) dominated in *COI* identification, and *Crassostrea gigas* (Mollusca), *Arcuatula senhousia* (Mollusca), and *Halosydna brevisetosa* (Annelida) were the most abundant in *18S rRNA* identification. Designing specific markers to track important fouling species is strongly recommended (Marshall and Stepien, 2019). For instance, targeted markers were successfully used to detect the quagga mussel in the Rhine River harbor of Basel (De Ventura *et al.*, 2017) and zebra mussel in the Red River off Lake Winnipeg (Gingera *et al.*, 2017), both of which were missed by traditional morphological monitoring. Therefore, we suggest employing complementary targeted metabarcoding assay to monitor dominant macrofouling species in this region for future monitoring efforts.

### 4.2 Changes in Taxonomic Diversity and Biofouling Community

Both morphological and *COI* data revealed similar patterns of change in the diversity and community structure of the fouling species in the present study, with these changes being significantly influenced by sampling date. Regarding the changes in biodiversity of fouling organisms attached to the nets, the diversity and richness indices on June 27 were relatively low compared to those on other sampling dates. We suggest that the appearance of *E. crocea* was a key factor leading to this shift, as hydrozoans are often the first colonizers on mesh nets, significantly affecting subsequent biodiversity and species richness (Bloecher *et al*., 2013; Xie *et al*., 2019). The presence of *E. crocea* led to the replacement of previously attached organisms, resulting in a decrease in diversity. However, as *E. crocea* and *Caprella* sp. covered most of the nets, the numbers of other fouling organisms began to increase, causing an increase in both species diversity and richness, with evenness also stabilizing. These results are consistent with our observations on the nets. Beta diversity analysis revealed significant differences in community composition between May 30 to June 13 and June 21 to July 20, and *E. crocea*, *Caprella* sp., *M. edulis*, and *J. marmorata* contributed significantly to community variation. These results further support the idea that the arising of hydrozoans and amphipoda at the end of June represented a crucial turning point in the structural changes of fouling organism communities in this region. A hanging panel experiment at Beiguan Port in the East China Sea also revealed similar phenomena (Li *et al*., 2018). We suggest that implementing targeted interventions for these key species at the beginning of summer may help to reduce the impact of fouling organisms on net cages in this region.

For water eDNA metabarcoding, the trend in diversity changes for the *COI* marker closely mirrored the morphological results. Unlike morphological diversity, however, the lowest points for *COI* diversity and richness occurred on June 13, which was earlier than observed in the morphological results. Beta diversity analysis with *COI* sequence also indicated that June 13 and June 27 formed distinct clusters, separating this group from the preceding and subsequent samples, suggesting that changes in species composition and diversity occurred during this period, leading to the shifts in community structure. In addition to these trends, we also noted that water eDNA metabarcoding detected abundance peaks for some biofouling species earlier than those from morphological observations. For example, the maximum abundance of *J. marmorata* was observed on June 21, but was detected on June 13 with *COI*, and on May 30 with *18S rRNA*. Similarly, the maximum abundance of *H. brevisetosa* occurred on July 14, but was detected on June 27 with both *COI* and *18S rRNA* markers. For *A. senhousia*, the peak abundance was observed on July 20, while with *COI* and *18S rRNA*, it was detected on July 14. The early detection of metabarcoding for biofouling species has been well-documented (De Ventura *et al*., 2017; Gingera *et al*., 2017; Marshall and Stepien, 2019). Thus, we propose that water eDNA metabarcoding could be a valuable tool for informing preventative management decision (*e.g*., timing of treatment), potentially reducing the costs associated with biofouling management in this region.

Two main factors might lead to the observed divergent temporal trends in diversity indices in *COI* and morphological datasets. First, methodological limitations in metabarcoding (*e.g*., primer bias, the completeness of reference databases) may result in incomplete or inaccurate detection of certain taxa. As discussed above, these limitations could contribute to temporal inconsistencies in the observed patterns of diversity change. Second, there is a temporal lag between the diversity patterns captured by eDNA from water samples and those observed in morphology on mesh nets. Most macrofoulers experience a planktonic phase before settlement, potentially allowing eDNA to detect their presence in the water column ahead of their physical attachment to the nets. For example, the earlier detection of *J. marmorata* in seawater than on mesh nets could contribute to its planktonic phase (Franz and Mohamed, 1989). Similar methodological lag effects have also been reported in other studies. For instance, some planktonic organisms exhibit significant lagged effects on fish gill health, highlighting the importance of understanding ecological processes during the planktonic phase of marine species (Algueró Muñiz *et al*., 2024).

## 5 Conclusions

eDNA from water samples is, to some extent, indicative of the presence and temporal changes in the diversity of macrofoulers on cage nets, as detected by traditional morphological method, in the coastal area of the Yellow Sea. The appearance of *E. crocea* and *Caprella* sp. at the end of June marked a substantial turning point in the change of biofouling communities. Future studies could design targeted primers for these key fouling species to improve monitoring efficiency.

## Supplementary Materials

Supplementary materials are available in the online version of this article at https://doi.org/10.1007/s11802-025-6168-5.

## Acknowledgements

This work was supported by grants from the National Key Research and Development Program of China (No. 2023YFD2401103), and the Fundamental Research Funds for the Central Universities.

## Author Contributions

Yalan Gu: performed research, analyzed data, wrote the paper. Jie Wang: designed research, wrote and reviewed

the paper. Yunwei Dong: designed research, reviewed the paper.

## Data Availability

The data and references presented in this study are available from the corresponding author upon request.

## Declarations

### Ethics Approval and Consent to Participate

The present study was performed according to the standard operation procedures (SOPs) of the Guide for the Use of Experimental Animals of the Ocean University of China. All animal care and use procedures were approved by the Institutional Animal Care and Use Committee of Ocean University of China.

### Consent for Publication

Informed consent for publication was obtained from all participants.

### Conflict of Interests

The authors declare that they have no conflict of interests. Yunwei Dong is one of the Editorial Board Members, but he was not involved in the journal's review of, or decision related to, this manuscript.

### Open Access



## References

Algueró Muñiz, M., Spatharis, S., Dwyer, T., De Noia, M., Cheaib, B., Liu, Y. W., *et al*., 2024. High-resolution longitudinal eDNA metabarcoding and morphological tracking of planktonic threats to *Salmon* aquaculture. *Environmental DNA*, **6** (5): e70005.

Ammon, U. V., Wood, S. A., Laroche, O., Zaiko, A., Tait, L., Lavery, S., *et al*., 2018. Combining morpho-taxonomy and metabarcoding enhances the detection of non-indigenous marine pests in biofouling communities. *Scientific Reports*, **8** (1): 16290.

Atalah, J., Newcombe, E. M., Hopkins, G. A., and Forrest, B. M., 2014. Potential biocontrol agents for biofouling on artificial structures. *Biofouling*, **30** (8): 999–1010.

Azevedo, J., Antunes, J. T., Machado, A. M., Vasconcelos, V., Leão, P. N., and Froufe, E., 2020. Monitoring of biofouling communities in a Portuguese port using a combined morphological and metabarcoding approach. *Scientific Reports*, **10** (1): 13461.

Beng, K. C., and Corlett, R. T., 2020. Applications of environmental DNA (eDNA) in ecology and conservation: Opportunities, challenges and prospects. *Biodiversity and Conservation*, **29** (7): 2089–2121.

Beveridge, M. C. M., 2004. *Cage Aquaculture*. 3rd edition. Blackwell Publishing, Oxford, 368pp.

Bloecher, N., Olsen, Y., and Guenther, J., 2013. Variability of biofouling communities on fish cage nets: A 1-year field study at a Norwegian salmon farm. *Aquaculture*, **416**: 302–309.

Bourlat, S. J., Borja, A., Gilbert, J., Taylor, M. I., Davies, N., Weisberg, S. B., *et al*., 2013. Genomics in marine monitoring: New opportunities for assessing marine health status. *Marine Pollution Bulletin*, **74** (1): 19–31.

Briand, J. F., Pochon, X., Wood, S. A., Bressy, C., Garnier, C., Réhel, K., *et al*., 2018. Metabarcoding and metabolomics offer complementarity in deciphering marine eukaryotic biofouling community shifts. *Biofouling*, **34** (6): 657–672.

Castro-Cubillos, M. L., Taylor, J. D., Mastretta-Yanes, A., Benítez-Villalobos, F., and Islas-Villanueva, V., 2022. Monitoring of benthic eukaryotic communities in two tropical coastal lagoons through eDNA metabarcoding: A spatial and temporal approximation. *Scientific Reports*, **12** (1): 10089.

Chen, Q. P., Bi, C. W., Zhang, Z. X., and Zhao, Y. P., 2023. Hydrodynamic effect of different biofouling types on aquaculture netting. *Ocean Engineering*, **279**: 114430.

Cowart, D. A., Pinheiro, M., Mouchel, O., Maguer, M., Grall, J., Miné, J., *et al*., 2015. Metabarcoding is powerful yet still blind: A comparative analysis of morphological and molecular surveys of seagrass communities. *PLoS One*, **10** (2): e0117562.

De Ventura, L., Kopp, K., Seppälä, K., and Jokela, J., 2017. Tracing the quagga mussel invasion along the Rhine river system using eDNA markers: Early detection and surveillance of invasive zebra and quagga mussels. *Management of Biological Invasions*, **8** (1): 101–112.

Deiner, K., Fronhofer, E. A., Mächler, E., Walser, J. C., and Altermatt, F., 2016. Environmental DNA reveals that rivers are conveyer belts of biodiversity information. *Nature Communications*, **7** (1): 12544.

Djurhuus, A., Closek, C. J., Kelly, R. P., Pitz, K. J., Michisaki, R. P., Starks, H. A., *et al*., 2020. Environmental DNA reveals seasonal shifts and potential interactions in a marine community. *Nature Communications*, **11** (1): 254.

Dürr, S., and Watson, D. I., 2010. *Biofouling and Antifouling in Aquaculture*. Blackwell Publishing, Oxford, 267–287.

Edgar, R. C., 2016. UNOISE2: Improved error-correction for Illumina 16S and ITS amplicon sequencing. *bioRxiv*, 081257.

Elbrecht, V., Vamos, E. E., Meissner, K., Aroviita, J., and Leese, F., 2017. Assessing strengths and weaknesses of DNA metabarcoding-based macroinvertebrate identification for routine stream monitoring. *Methods in Ecology and Evolution*, **8** (10): 1265–1275.

Fishery Bureau of Ministry of Agriculture of the People's Republic of China, 2024. *China Fishery Statistical Yearbook*. China Agriculture Press, Beijing, 21–29.

Fitridge, I., Dempster, T., Guenther, J., and de Nys, R., 2012. The impact and control of biofouling in marine aquaculture:

A review. *Biofouling*, **28** (7): 649–669.
Fleming, J. F., 2023. The wealth of shared resources: Improving molecular taxonomy using eDNA and public databases. *Zoologica Scripta*, **52** (3): 226–234.
Fletcher, L. M., Zaiko, A., Atalah, J., Richter, I., Dufour, C. M., Pochon, X., *et al*., 2017. Bilge water as a vector for the spread of marine pests: A morphological, metabarcoding and experimental assessment. *Biological Invasions*, **19**: 2851–2867.
Franz, D. R., and Mohamed, Y., 1989. Short-distance dispersal in a fouling community amphipod crustacean, *Jassa marmorata* Holmes. *Journal of Experimental Marine Biology and Ecology*, **133** (1–2): 1–13.
Frontalini, F., Greco, M., Di Bella, L., Lejzerowicz, F., Reo, E., Caruso, A., *et al*., 2018. Assessing the effect of mercury pollution on cultured benthic foraminifera community using morphological and eDNA metabarcoding approaches. *Marine Pollution Bulletin*, **129** (2): 512–524.
Gao, Q. F., and Dong, S. L., 2023. Cage farming of fish in open waters. In: *Aquaculture Ecology*. Dong, S. L., *et al*., eds., Springer Nature, Singapore, 425–445.
Gingera, T. D., Bajno, R., Docker, M. F., and Reist, J. D., 2017. Environmental DNA as a detection tool for zebra mussels *Dreissena polymorpha* (Pallas, 1771) at the forefront of an invasion event in Lake Winnipeg, Manitoba, Canada. *Management of Biological Invasions*, **8** (3): 287–300.
Hajibabaei, M., Porter, T. M., Wright, M., and Rudar, J., 2019. *COI* metabarcoding primer choice affects richness and recovery of indicator taxa in freshwater systems. *PLoS One*, **14** (9): e0220953.
Hanžek, N., Udovič, M. G., Kajan, K., Borics, G., Várbíró, G., Stoeck, T., *et al*., 2021. Assessing ecological status in karstic lakes through the integration of phytoplankton functional groups, morphological approach and environmental DNA metabarcoding. *Ecological Indicators*, **131**: 108166.
He, X., Sutherland, T. F., Pawlowski, J., and Abbott, C. L., 2019. Responses of foraminifera communities to aquaculture-derived organic enrichment as revealed by environmental DNA metabarcoding. *Molecular Ecology*, **28** (5): 1138–1153.
Kassambara, A., 2023. rstatix: Pipe-friendly framework for basic statistical tests (R package version 0.7.2). https://github.com/kassambara/rstatix.
Kelly, R. P., Shelton, A. O., and Gallego, R., 2019. Understanding PCR processes to draw meaningful conclusions from environmental DNA studies. *Scientific Reports*, **9** (1): 12133.
Lanzén, A., Dahlgren, T. G., Bagi, A., and Hestetun, J. T., 2021. Benthic eDNA metabarcoding provides accurate assessments of impact from oil extraction, and ecological insights. *Ecological Indicators*, **130**: 108064.
Leray, M., Yang, J. Y., Meyer, C. P., Mills, S. C., Agudelo, N., Ranwez, V., *et al*., 2013. A new versatile primer set targeting a short fragment of the mitochondrial *COI* region for metabarcoding metazoan diversity: Application for characterizing coral reef fish gut contents. *Frontiers in Zoology*, **10**: 1–14.
Li, Z., Lin, H. S., Huang, Y. Q., He, X. B., Lin, J. H., Liu, K., *et al*., 2018. Community structure of fouling organisms and its major impact factors in the Beiguan Port, China. *Haiyang Xuebao*, **40** (12): 81–93.
Liu, Y. X., Chen, L., Ma, T., Li, X., Zheng, M., Zhou, X., *et al*., 2023. EasyAmplicon: An easy-to-use, open-source, reproducible, and community-based pipeline for amplicon data analysis in microbiome research. *iMeta*, **2** (1): e83.
Marshall, N. T., and Stepien, C. A., 2019. Invasion genetics from eDNA and thousands of larvae: A targeted metabarcoding assay that distinguishes species and population variation of zebra and quagga mussels. *Ecology and Evolution*, **9** (6): 3515–3538.
Meyer, C. P., 2003. Molecular systematics of cowries (Gastropoda: Cypraeidae) and diversification patterns in the tropics. *Biological Journal of the Linnean Society*, **79** (3): 401–459.
Oksanen, J., Simpson, G. L., Blanchet, F. G., Kindt, R., Legendre, P., Minchin, P. R., *et al*., 2022. vegan: Community ecology package (R package version 2.6-4). https://CRAN.R-project.org/package=vegan.
Pawlowski, J., Esling, P., Lejzerowicz, F., Cedhagen, T., and Wilding, T. A., 2014. Environmental monitoring through protist next-generation sequencing metabarcoding: Assessing the impact of fish farming on benthic foraminifera communities. *Molecular Ecology Resources*, **14** (6): 1129–1140.
Pinna, M., Zangaro, F., and Specchia, V., 2024. Assessing benthic macroinvertebrate communities' spatial heterogeneity in Mediterranean transitional waters through eDNA metabarcoding. *Scientific Reports*, **14** (1): 17890.
Portas, A., Quillien, N., Culioli, G., and Briand, J. F., 2022. Eukaryotic diversity of marine biofouling from coastal to offshore areas. *Frontiers in Marine Science*, **9**: 971939.
R Core Team, 2024. R: A language and environment for statistical computing. https://www.R-project.org/.
Rees, H. C., Maddison, B. C., Middleditch, D. J., Patmore, J. R. M., Gough, K. C., and Crispo, E., 2014. Review: The detection of aquatic animal species using environmental DNA–A review of eDNA as a survey tool in ecology. *Journal of Applied Ecology*, **51** (5): 1450–1459.
Rey, A., Basurko, O. C., and Rodriguez-Ezpeleta, N., 2020. Considerations for metabarcoding-based port biological baseline surveys aimed at marine nonindigenous species monitoring and risk assessments. *Ecology and Evolution*, **10** (5): 2452–2465.
Rognes, T., Flouri, T., Nichols, B., Quince, C., and Mahé, F., 2016. VSEARCH: A versatile open source tool for metagenomics. *PeerJ*, **4**: e2584.
Ross, K. A., Thorpe, J. P., and Brand, A. R., 2004. Biological control of fouling in suspended scallop cultivation. *Aquaculture*, **229** (1–4): 99–116.
Roussel, J., Paillisson, J., Tréguier, A., and Petit, E., 2015. The downside of eDNA as a survey tool in water bodies. *Journal of Applied Ecology*, **52** (4): 823–826.
Salama, A. J., Satheesh, S., and Balqadi, A. A., 2018. Development of biofouling communities on nylon net panels submerged in the central Red Sea: Effects of season and depth. *Thalassas: An International Journal of Marine Sciences*, **34**: 199–208.
Subías-Baratau, A., Sanchez-Vidal, A., Di Martino, E., and Figuerola, B., 2022. Marine biofouling organisms on beached, buoyant and benthic plastic debris in the Catalan Sea. *Marine Pollution Bulletin*, **175**: 113405.
van der Loos, L. M., and Nijland, R., 2021. Biases in bulk: DNA metabarcoding of marine communities and the methodology involved. *Molecular Ecology*, **30** (13): 3270–3288.
Xie, B., Wu, J., and Huang, L., 2019. Temporal and spatial variations of macrofouling organisms on ecological floating beds in Yundang Lagoon, China. *Marine Pollution Bulletin*, **148**: 156–167.
Yan, T., and Cao, W. H., 2008. Ecology of marine fouling organism in Huanghai and Bohai Seas. *Journal of Marine Sciences*, **3**: 109–120.
Yang, Z., Bai, X., Jiang, H., and Yuan, C., 2016. Analysis of biofouling occurrence trends on ship hull surface. *Ship Engineering*, **38** (2): 29–33.

Zaiko, A., Schimanski, K., Pochon, X., Hopkins, G. A., Goldstien, S., Floerl, O., *et al*., 2016. Metabarcoding improves detection of eukaryotes from early biofouling communities: Implications for pest monitoring and pathway management. *Biofouling*, **32** (6): 671–684.

Zhang, H., and Lin, S., 2005. Development of a *cob*-18S rRNA gene real-time PCR assay for quantifying *Pfiesteria shumwayae* in the natural environment. *Applied and Environmental Microbiology*, **71** (11): 7053–7063.

Zhou, J. L., Liu, L., Wang, X. F., and Fu, J. R., 2021. The research progress of fouling organisms in coastal waters of China is reviewed. *Forum of South China*, **52** (10): 27–32.

Zhou, S. B., Li, Z. Q., Peng, S. C., Zhang, D. J., Li, W. C., Hong, M. Y., *et al*., 2022. Combining eDNA and morphological approaches to reveal the impacts of long-term discharges of shale gas wastewaters on receiving waters. *Water Research*, **222**: 118869.

**(Edited by Qiu Yantao)**